Available online at www.sciencedirect.com

SciVerse ScienceDirect

www.elsevier.com/locate/matchar

Study of phase decomposition and coarsening of γ′ precipitates in Ni-12 at.% Ti alloy

C.G. Garay-Reyes[a,*], F. Hernández-Santiago[b], N. Cayetano-Castro[c], V.M. López-Hirata[d], J. García-Rocha[a], J.L. Hernández-Rivera[e], H.J. Dorantes-Rosales[d], J.J. Cruz-Rivera[a]

[a]Universidad Autónoma de San Luis Potosí, Instituto de Metalurgia, Sierra leona 550, Col. Lomas 2 sección, 78210 S.L.P., Mexico
[b]Instituto Politécnico Nacional, ESIME-AZC, Av. de las Granjas 682, col. Sta. Catarina, 02550 D.F., Mexico
[c]Instituto Potosino de Investigación Científica y Tecnológica, División de Materiales Avanzados, camino a la Presa San José 2055, Col Lomas 4 sección, 78216 S.L.P., Mexico
[d]Instituto Politécnico Nacional, ESIQIE-DIM, 118-556, D.F., Mexico
[e]Centro de Investigación de Materiales Avanzados (CIMAV), Laboratorio Nacional de Nanotecnología, Miguel de Cervantes 120, 31109 Chihuahua, Mexico

ARTICLE DATA

Article history:
Received 13 April 2013
Received in revised form 24 May 2013
Accepted 30 May 2013

Keywords:
Nickel based superalloys
Spinodal conditional
Morphological evolution
γ′ precipitates coarsening
TIDC theory
LSW theory

ABSTRACT

The early stages of phase decomposition, morphological evolution of precipitates, coarsening kinetics of γ′ precipitates and micro-hardness in Ni-12 at.% Ti alloy are studied by transmission electron microscopy (TEM) and Vickers hardness tests (VHN). Disk-shaped specimens are solution treated at 1473 K (1200 °C) and aged at 823, 923 and 1023 K (550, 650 and 750 °C) during several periods of time. TEM results show that a conditional spinodal of order occurs at the beginning of the phase decomposition and exhibit the following decomposition sequence and morphological evolution of precipitates: $\alpha_{sss} \rightarrow \gamma''$ irregular–cuboidal + $\gamma_s \rightarrow \gamma'$ cuboidal–parallelepiped + $\gamma \rightarrow \eta$ plates + γ. In general during the coarsening of γ′ precipitates, the experimental coarsening kinetics do not fit well to the LSW or TIDC ($n = 2.281$) theoretical models, however the activation energies determined using the TIDC and LSW theories (262.846 and 283.6075 kJ mol^{-1}, respectively) are consistent with previously reported values. The highest hardness obtained at 823, 923 and 1023 K (550, 650 and 750 °C) is associated with the presence of γ′ precipitates.

1. Introduction

Solid state precipitation is one of the most efficient ways to develop desirable microstructures for advanced engineering materials, such as nickel-based superalloys that are primarily used in the applications which require high-temperature strength. The rich-Ni Ni–Ti system has been studied by many researchers who used many different techniques including magnetic measurements, X-ray diffraction (XRD), transmission electron microscopy (TEM), high-resolution TEM (HR-TEM), atom-probe field-ion microscopy (AP-FIM) and small-angle neutron scattering (SANS) [1–16]. The above mentioned studies have concluded that cuboidal-type γ′ precipitates ($L1_2$ structure) aligned along <100> directions with faces parallel to {100} planes are the cause of hardening. There has also been an evidence of two metastable states (γ″ and γ′) before the formation of η stable phase, however, the relationship between

* *Corresponding author at: Universidad Autónoma de San Luis Potosí, Instituto de Metalurgia, Sierra leona 550, Col.* Lomas 2 sección, C.P. 78210, San Luis Potosí, S.L.P., Mexico. Tel./fax: +52 4448254583.
E-mail address: garay_820123@hotmail.com (C.G. Garay-Reyes).

1044-5803/$ – see front matter © 2013 Published by Elsevier Inc.
http://dx.doi.org/10.1016/j.matchar.2013.05.017

the ordering and the spinodal decomposition in the early stage of decomposition is not yet clear. It is mentioned that during the early stage of phase decomposition there are at least two ways to obtain a two phase mixture (γ and γ′) from the supersaturated solid solution (α_{sss}). In the first case, α_{sss} is unstable with respect to phase separation and spontaneously form rich-Ti and lean-Ti disordered regions, ordering within the rich-Ti regions occurs close to stoichiometric composition (Ni_3Ti), it is called 'spinodal-clustering' [10] with the following decomposition sequence:

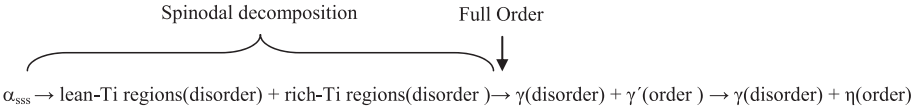

In the second case, the α_{sss} is unstable with respect to ordering and this in turn, is unstable with respect to spinodal decomposition, this is called 'conditional spinodal' [5–7,14–16] and follows the phase decomposition sequence:

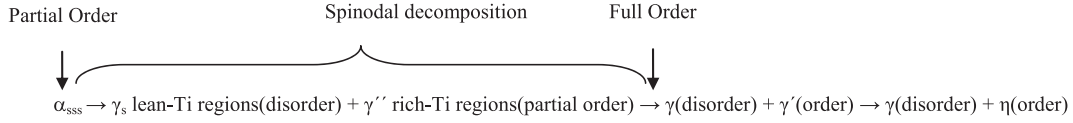

On the other hand, high-temperatures and prolonged service times could originate coarsening of γ′ precipitates causing loss of coherency which may eventually affect the mechanical properties. Coarsening is theoretically described by the model proposed by Lifshitz–Slyozov and Wagner (LSW theory) [17,18] which predicts coarsening of precipitates dispersed in a fluid matrix according to the relationship, $r^3 = kt$ for diffusion-controlled coarsening, where r is the average radius of the precipitate, t is the aging time and k is the coarsening rate constant. The assumptions of this model are the following: a) the system is a fluid, b) the volume fraction (f_v) of the precipitates is relatively low so that the diffusion fields of precipitates do not overlap, c) precipitates are spherical and d) there are no elastic strains in the interface matrix/precipitate. There exists some modifications to the LSW theory [19–26] that take into account the effect of f_v, $k = k(f_v)$, all of these theories evidenced a broadening of the particle size distribution (PSD) and increase in the coarsening rate constant with an increase in the volume fraction of the precipitates, however, was evident a linear relationship between the cube of the average radius and aging time similar to LSW theory. A different behavior of coarsening to that observed in fluid systems has been reported for Ni-based superalloys with elastic strains [27–32], where constant k decreases as a function of f_v which is known as anomalous coarsening. A more realistic model where coarsening kinetics are independent f_v has been developed by Ardell–Ozolins [33] and Ardell [34] and is called trans-interface diffusion-controlled (TIDC) theory. The TIDC theory assumes that: i) diffusion in an ordered phase is much slower than in a disordered phase and ii) the interface between matrix/precipitate is ragged, not smooth. A rate law of type $\langle r\rangle^n \approx kt$ is predicted by the TIDC theory, where n is related to the width of the interface matrix/precipitate. The coarsening kinetics of rich-Ni Ni–Ti system has been studied in γ″ and γ′ precipitates. Different growth exponents of γ″ precipitates have been reported for instance at $t^{0.21}$ [13] and between $t^{0.21}$ and $t^{0.30}$ [14]. Values of $t^{0.33}$ [8], $t^{0.23}$ [12], from $t^{0.25}$ to $t^{0.33}$ [9] and between $t^{0.34}$ and $t^{0.42}$ [14] were found in γ′ precipitates. In studies relating to γ′ precipitates based on the TIDC theory, an exponent $n = 2.375$ was initially used [35], but a subsequent study evidenced with an exponent $n = 2.281$ is the best fit[36]. Therefore, the main objectives of the present investigation are to obtain evidence of the relationship between ordering and decomposition spinodal, to evaluate the morphological evolution of precipitates, to determine which model (LSW or the TIDC) has the best fit to the coarsening of γ′ precipitates, to determine the activation energy by both models and to evaluate the mechanical behavior by micro-hardness tests.

2. Experimental Procedure

Buttons of 10 g of Ni-12 at.% Ti alloy were obtained by melting from electrolytic Ni (99.99%) and Ti sponge (99.99%) under a high purity argon atmosphere using an electric-arc furnace. Buttons were homogenized in quartz tubes under an argon atmosphere at 1473 K (1200 °C) for 168 h. Disk-shaped specimens of around 2 mm in thickness and 1 cm of diameter were cut from the homogenized buttons and then were solution treated at 1473 K (1200 °C) for 4 h, quenched in ice-water and finally aged at 823, 923 and 1023 K (550, 650 and 750 °C) for several periods of time (5 to 50,000 min). Vickers micro-hardness measurements were performed using a 100 g load with 15 s dwell time and 20 indentations were made on each sample. Disk-shaped specimens used for TEM analysis were grounded to a thickness of 0.10 mm and then punched to obtain disk-shaped samples of 3 mm in diameter. The resulting specimens were thinned by the twin-jet electropolishing method at 223 K (−50 °C) into an electrolyte composed by 30% of HNO_3 and 70% of methanol. Microstructural characterization was carried out in a JEOL JEM-1230 transmission electron microscope operated at 100 kV equipped

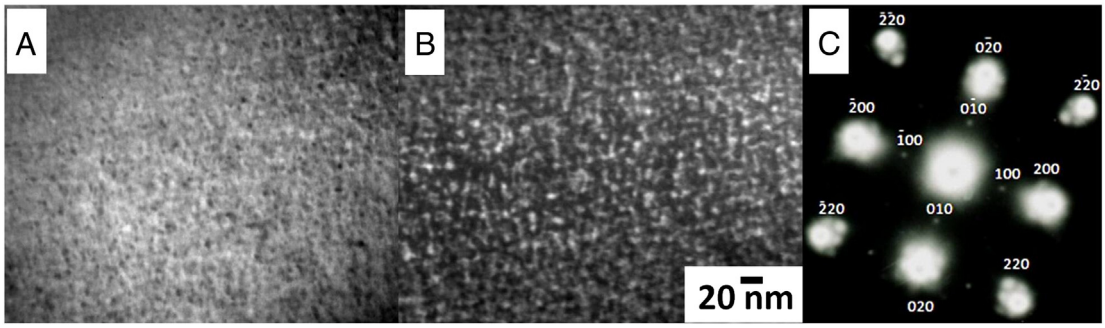

Fig. 1 – A) Bright-field and B) Dark-field transmission electron micrographs and C) corresponding diffraction pattern obtained in Ni-12 at.% Ti alloy after quenching.

with a CCD camera and an energy dispersive spectrometer (EDS). The size of precipitates was measured from dark-field transmission electron micrographs acquired from selected area diffraction patterns in the condition of two-beam using a 100 superlattice reflection. Around 800 precipitates in each sample were considered for the measurements in order to have a representative statistical value.

3. Results and Discussion

3.1. *Early-stage of Decomposition*

The bright-field and dark-field TEM micrographs presented in Fig. 1A and B, respectively, were obtained after quenching. It is observed that a modulated structure with a homogeneous distribution of irregular-type precipitates with a diffuse matrix/precipitate interface, which is a characteristic of spinodal decomposition [5–11,13–16]. The TEM diffraction pattern presented in Fig. 1C gives evidence of the coexistence of 100 superlattice reflections and diffuse satellites around the 220 and 200 reflections characteristics of ordering and of spinodal decomposition, respectively. It evidences a first stage in which the total energy of α_{sss} decreases due to a partial order that subsequently leads to spinodal decomposition, i.e. 'conditional spinodal' [5–7,14–16].

3.2. *Morphological Evolution of Precipitates*

The morphological evolution of precipitates in anisotropic solid two-phase systems such as in the Ni-12 at.% Ti alloy depends on the interplay between elastic and interfacial energies [37]. In the present study a strong temperature dependence on the morphological evolution is observed. Initially, γ″ precipitates exhibit irregular-type morphology, when the volume of these precipitates increases the elastic energy becomes important and precipitates evolve to cuboidal-type morphology with rounded corners. It has been reported that in this stage γ″ cuboidal-type precipitates (<3 nm) achieve a close to stoichiometric chemical composition (Ni_3Ti) and then evolve to γ′ cuboidal-type precipitates (>3 nm) aligned along the <100> directions [12,14–16]. Subsequently, the morphology of cuboidal-type γ′ precipitates evolve to a parallelepiped-type aligned along the <100> directions. Finally they adopt the plate-type morphology which corresponds to η phase, which grows on the (111) plane of the matrix phase (see Fig. 2) [7,8,11]. Thus, the decomposition and microstructural evolving sequences are presented in Fig. 3:

3.3. *Coarsening Kinetics of γ′ Precipitates*

3.3.1. *Particle Size Distribution (PSD)*

The experimental PSDs determined from dark-field TEM micrographs are compared with the theoretical distributions, LSW and TIDC (n = 2.281 [36]) theories (Fig. 4). The LSW theory for diffusion-controlled coarsening leads to a highly asymmetric PSD with a cutoff near the particle radius (ρ = 1), the TIDC distribution is based entirely on the n parameter [35] and is closer to theoretical distribution of LSW theory for the interface-controlled coarsening, where the PSD is more symmetrical compared to PSD of the LSW theory for diffusion-controlled coarsening. To determine the experimental PSDs, the equivalent radius of a sphere with equal volume was used as size parameter of the cuboidal precipitates and the probability density ($\rho^2 f(\rho)$) is determined with the following equation [38]:

$$\rho^2 f(\rho) = \frac{N_i(r, r+\Delta r)}{\sum N_i(r, r+\Delta r)} \frac{\bar{r}}{\Delta r} \quad (1)$$

where $\bar{r}$ is the average radius of the precipitates and $N_i(r, r + \Delta r)$ represents the number of precipitates in a given class interval Δr. The normalized radii (ρ) is defined as the ratio of $r/\bar{r}$. In general, the experimental PSDs do not fit well to the LSW or TIDC theoretical distributions, but a slight broadening and a decrease of probability density in the experimental PSDs at long aging times was observed. The LSW theoretical distribution is independent of aging time with a volume fraction close to zero and the TIDC theoretical distribution is dependent on the amplitude of the interface, which varies according to the radius of the precipitates and is independent of the volume fraction, it should be noted that both LSW and TIDC theories do not take into account elastic strain, therefore it can be inferred that the slight broadening and the decrease of probability density presents contributions of volume fraction and elastic strain, because experimental PSDs broad and symmetrical generally can only be explained by elastic strain [8,39] and high volume fraction [19–25].

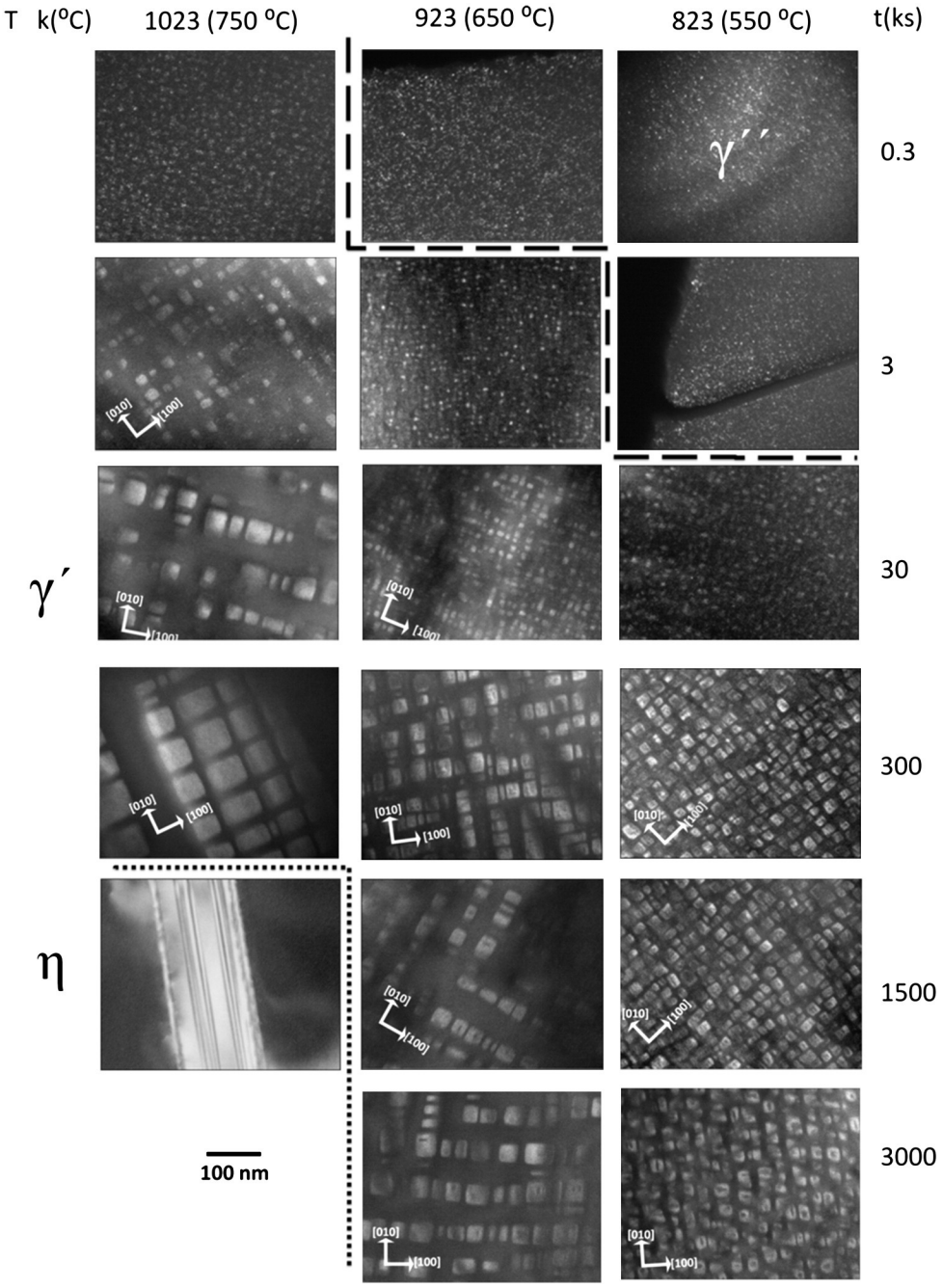

Fig. 2 – Dark-field TEM micrographs showing the effects of *T* and *t* on the morphology of phases present in Ni-12 at.% Ti alloy, which are indicated by dotted lines.

3.3.2. *LSW and TIDC Theories*

Plots of r^3 vs t (LSW theory) and $r^{2.281}$ vs t (TIDC theory) are presented in Fig. 5. It is seen that both r^3 and $r^{2.281}$, exhibit a linear behavior with t. The fit to linear dependence is represented by the calculated linear regression coefficient, R^2. At 1023 K (750 °C), the R^2 value indicates an approach to the TIDC theory, while at lower temperatures (823 and 923 K (550 and 650 °C)), an approach to LSW model is observed. From values obtained of R^2 a best linear fit at 823, 923 and 1023 K (550, 650 and 750 °C) is given with a value of $n = 2.123$, where the value of R^2 are 0.87961, 0.85068 and 0.98556 at 823, 923 and 1023 K (550, 650 and 750 °C) respectively, and it should be noted that a better fit occurs at high temperatures (923 and 1023 K (650 and 750 °C)). The coarsening rate constant (k) calculated using the slope of the linear regression shows strong temperature dependence as can be seen in Fig. 5.

3.3.3. *Activation Energy*

The activation energies (Q) obtained from the Arrhenius plot ($ln\ k$ vs $1/T$), for TIDC ($n = 2.281$ [36]) and LSW theories,

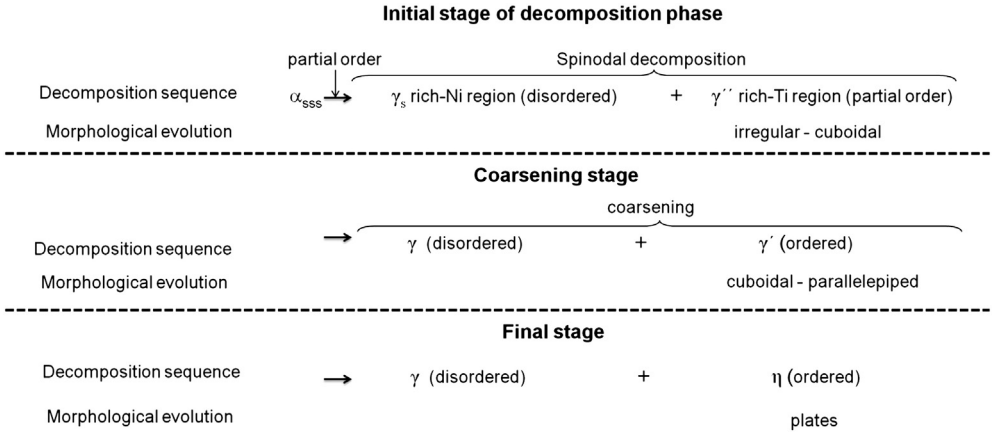

Fig. 3 – Decomposition sequence and morphological evolution in the Ni-12 at.% Ti alloy aged at different temperatures and times.

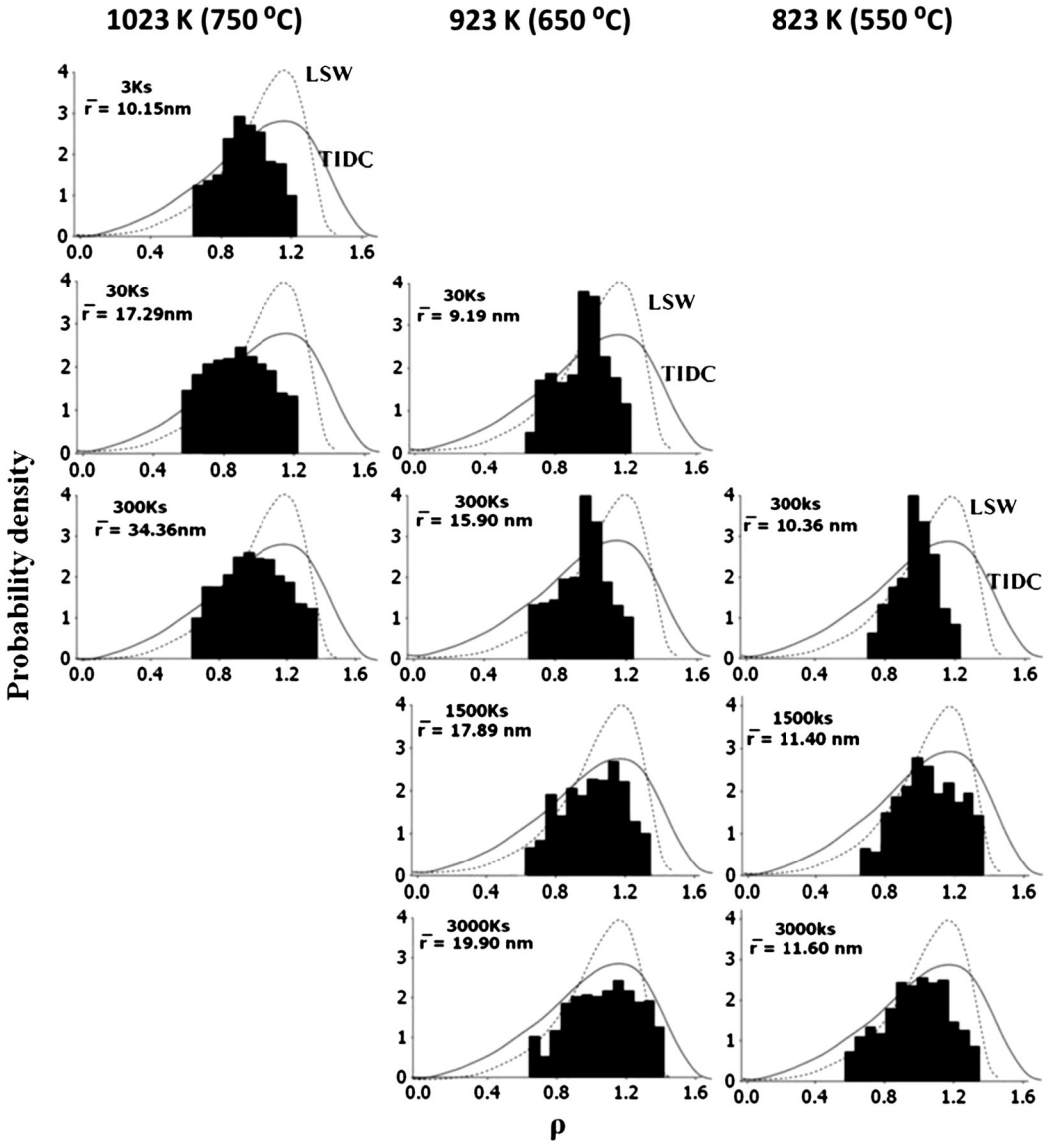

Fig. 4 – Comparison between the LSW (dotted gray line) and TIDC (solid black line—n = 2.281 [36]) theoretical distributions with the experimental PSDs of γ′ precipitates obtained at different aging temperatures and times.

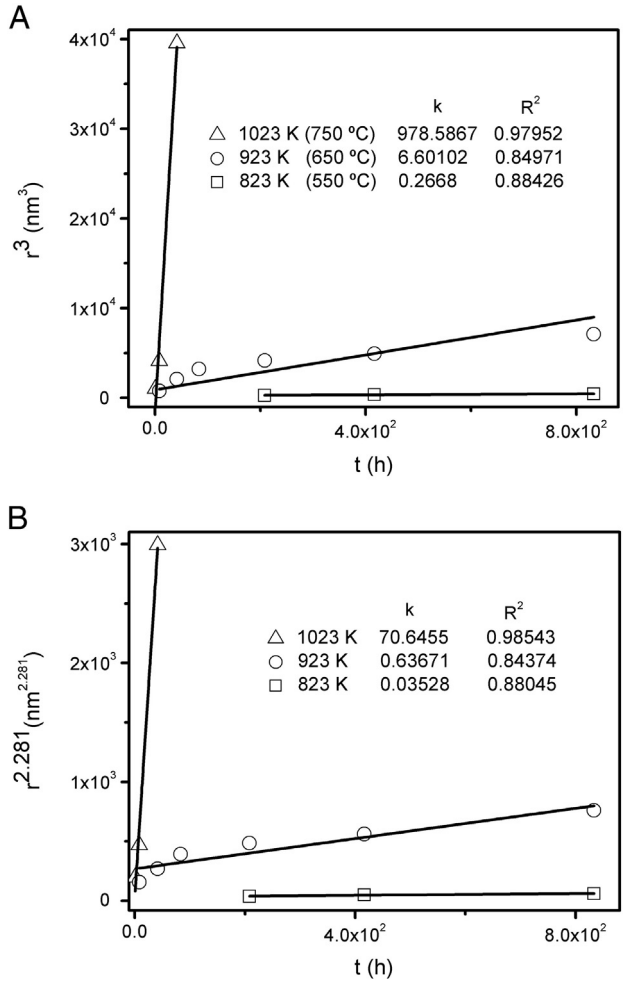

Fig. 5 – Plots of: A) r^3 vs t (LSW theory) and B) $r^{2.281}$ vs t (TIDC theory) of Ni-12 at.% Ti alloy aged at different temperatures.

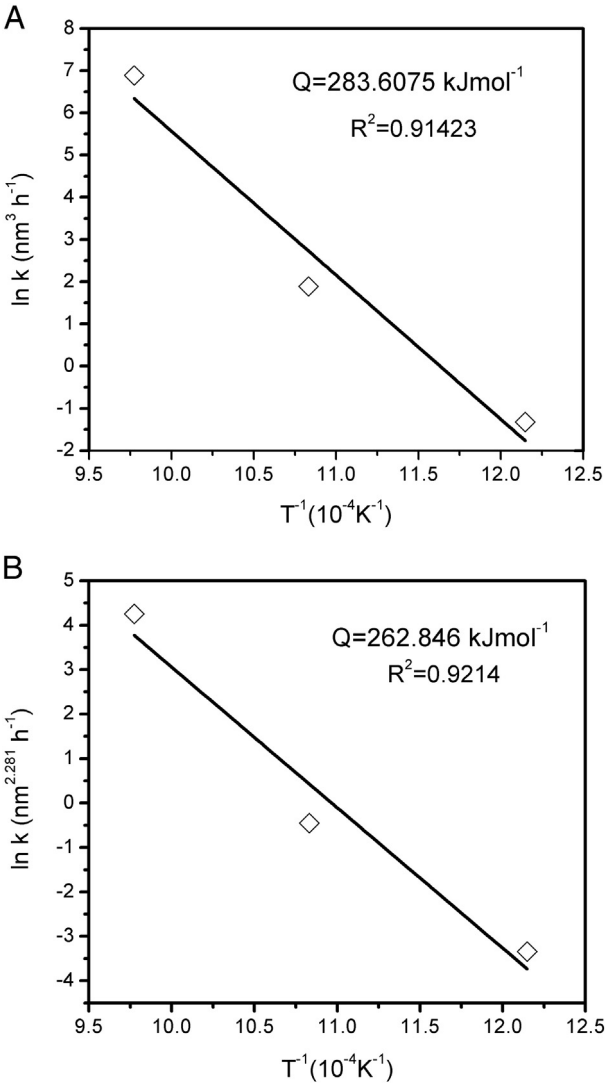

Fig. 6 – Plots of *ln k* vs 1/*T*: A) LSW theory and B) TIDC theory (*n* = 2.281 [36]) for Ni-12 at.% Ti alloy.

are 262.846 and 283.6075 kJ mol^{-1}, respectively (Fig. 6). The value obtained for the LSW theory has a good correlation with the value obtained by Ardell in Ni-10.5 at.% Ti alloy (282.4 kJ mol^{-1}) [8] and the value obtained for the TIDC theory has a good correlation with the value obtained by Swalin and Martin for diffusion of Ti in nickel matrix (256.8 kJ mol^{-1}) [40] (it should be noted on the difference in the type of diffusion coefficient). The value of Q obtained with a value of n = 2.123 is 258.78 kJ mol^{-1}.

3.4. *Hardening Behavior*

The age-hardening curves obtained at 823, 923 and 1023 K (550, 650 and 750 °C) are shown in Fig. 7. In general, the hardening effect is associated to the interaction between precipitates and elastic strain fields around them with dislocations. The softening effect is associated to coarsening and loss of coherency of precipitates [41]. The maximum hardness at 1023 and 923 K (750 and 650 °C) is achieved after 5 and 5000 min respectively. In contrast, the maximum hardness during aging at 823 K (550 °C) is not achieved even for the longest aging time (50,000 min). The maximum hardness observed for all of the temperatures investigated is associated with the presence of γ′ precipitates and an increase of hardness with the aging temperature decreases associated to increase in volume fraction of the precipitates. It is also observed that the age-hardening

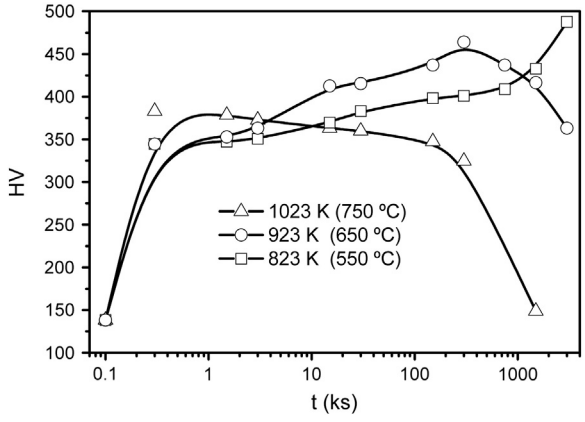

Fig. 7 – Age-hardening curves of Ni-12 at.% Ti alloy aged at different times and temperatures.

curves corresponding to temperatures of 923 and 823 K (650 and 550 °C) show two plateaus which according to Saito et al. [7] the first plateau indicates the presence of γ″ precipitates, while the second plateau the presence of γ′ precipitates.

4. Conclusions

From the results obtained it can be concluded that at the beginning of phase decomposition, ordering precedes spinodal decomposition. The morphological evolution of precipitates follows the sequence: $\alpha_{sss} \rightarrow \gamma''$ irregular–cuboidal + $\gamma_s \rightarrow \gamma'$ cuboidal–parallelepiped + $\gamma \rightarrow \eta$ plates + γ, with strong temperature dependence. In general during the coarsening of γ′ precipitates, the experimental coarsening kinetics do not fit well to the LSW or TIDC (n = 2.281) theoretical models, however the activation energies determined using the TIDC and LSW theories (262.846 and 283.6075 kJ mol^{-1}, respectively) are consistent with previously reported values. Finally, the maximum hardness obtained at 1023, 923 and 823 K (750, 650 and 550 °C), is associated with the presence of γ′ precipitates.

Acknowledgments

The technical assistance of Claudia Gpe. Elías Alfaro for TEM characterization is greatly appreciated. The first author would like to thank CONACYT for the scholarship given and extends a special acknowledgement to the Instituto de Metalurgia (UASLP) and Instituto Politécnico Nacional (IPN) for the facilities provided for performing the experimental work.

REFERENCES

[1] Taylor A, Floyd RW. The constitution of nickel-rich alloys of the nickel–chromium–aluminum system. J Inst Met 1952–53;81:25–32.
[2] Bagariatskii YA, Tiapkin YD. The mechanism of structure transformations in age hardening alloys based on nickel. Sov Phys Crystallogr 1957;2:414–21.
[3] Bagariatskii YA, Tiapkin YD. Fresh structural data on the decomposition of supersaturated solid solutions of titanium in nickel and nichrome. Sov Phys Crystallogr 1961;5:841–7.
[4] Bücle C, Genty B, Manenc J. Quelques aspects de la precipitation dans un alliage nickel-titane. Rev Metall 1959;56:247–59.
[5] Ben Israel DH, Fine ME. Precipitation studies in Ni-10 at.% Ti. Acta Metall 1963;11:1051–9.
[6] Sass SL, Mur T, Cohen JB. Diffraction contrast from non-spherical distortions—in particular a cuboidal inclusion. Philos Mag 1967;16:680–90.
[7] Saito K, Watanabe R. Precipitation in Ni-12 at.% Ti alloy. Jpn J Appl Phys 1969;8:14–23.
[8] Ardell AJ. The growth of gamma prime precipitates in aged Ni–Ti alloys. Metall Trans B 1970;1:525–34.
[9] Sinclair R, Leake JA, Ralph B. Spinodal decomposition of a nickel–titanium alloy. Phys Status Solidi A 1974;26:285–98.
[10] Laughlin DE. Spinodal decomposition in nickel based nickel–titanium alloys. Acta Metall 1976;24:53–8.
[11] Hashimoto K, Tsujimoto T. X-ray diffraction patterns and microstructures of aged Ni–Ti alloys. Trans JIM 1978;19:77–84.
[12] Grune R. Decomposition of Ni-12 at.% Ti by atom-probe field-ion microscopy. Acta Metall 1988;36:2797–809.
[13] Cerri A, Schönfeld B, Kostorz G. Decomposition kinetics in Ni–Ti alloys. Phys Rev B 1990;42:958–60.
[14] Vyskocil P, Pedersen JS, Kostorz G, Schönfeld B. Small-angle neutron scattering of precipitates in Ni-rich Ni–Ti alloys — I. Metastable states in poly- and single crystals. Acta Mater 1997;45:3311–8.
[15] Bucher R, Demè B, Heinrich H, Kohlbrecher J, Kompatscher M, Kostorz G, et al. In-situ neutron scattering studies of order and decomposition in Ni-rich Ni–Ti. Mater Sci Eng A 2002;324:77–81.
[16] Kompatscher M, Schönfeld B, Heinrich H, Kostorz G. Phase separation in Ni-rich Ni–Ti: the metastable states. Acta Mater 2003;51:165–75.
[17] Wagner C. Theorie der Alterung von Nierderschlägen durch Umlösen. Z Elektrochem 1961;65:581–94.
[18] Lifshitz IM, Slyozov VV. The kinetics of precipitation from supersaturated solid solutions. J Phys Chem Solids 1961;19:35–50.
[19] Ardell AJ. The effect of volume fraction on particle coarsening: theoretical considerations. Acta Metall 1972;20:61–71.
[20] Brailsford AD, Wynblatt P. The dependence of Ostwald ripening kinetics on particle volume fraction. Acta Metall 1979;27:489–97.
[21] Davies CKL, Nash P, Stevens RN. The effect of volume fraction of precipitate on Ostwald ripening. Acta Metall 1980;28: 179–89.
[22] Tsumaraya K, Miyata Y. Coarsening models incorporating both diffusion geometry and volume fraction of particles. Acta Metall 1983;31:437–52.
[23] Marqusee JA, Rose J. Kinetics of phase transitions: theory of Ostwald ripening. J Chem Phys 1984;80:536–43.
[24] Tokuyama M, Kawasaki K. Statistical–mechanical theory of coarsening of spherical droplets. Phys A 1984;123:386–411.
[25] Voorhees PW, Glicksman ME. Solution to the multi-particle diffusion problem with applications to Ostwald ripening — I. Theory. Acta Metall 1984;32:2001–12.
[26] Voorhees PW, Glicksman ME. Solution to the multi-particle diffusion problem with applications to Ostwald ripening — II. Computer simulations. Acta Metall 1984;32:2013–30.
[27] Kim DM, Ardell AJ. The volume-fraction dependence of Ni_3Ti coarsening kinetics—new evidence of anomalous behavior. Scr Mater 2000;43:381–4.
[28] Maheshwari A, Ardell AJ. Anomalous coarsening behavior of small volume fractions of Ni_3Al precipitates in binary Ni–Al alloys. Acta Metall Mater 1992;40:2661–7.
[29] Kim DM, Ardell AJ. Coarsening behavior of Ni_3Ga precipitates in Ni–Ga alloys: dependence of microstructure and kinetics on volume fraction. Metall Mater Trans A 2004;35:3063–9.
[30] Kim DM, Ardell AJ. Coarsening of Ni_3Ge in binary Ni–Ge alloys: microstructures and volume fraction dependence of kinetics. Acta Mater 2003;51:4073–82.
[31] Cho JH, Ardell AJ. Coarsening of Ni_3Si precipitates at volume fractions from 0.03 to 0.30. Acta Mater 1998;46: 5907–16.
[32] Ardell AJ. Observations on the effect of volume fraction on the coarsening of γ′ precipitates in binary Ni–Al alloys. Scr Metall Mater 1990;24:343–6.
[33] Ardell AJ, Ozolins V. Trans-interface diffusion-controlled coarsening. Nat Mater 2005;4:309–16.
[34] Ardell AJ. Quantitative predictions of the trans-interface diffusion-controlled theory of particle coarsening. Acta Mater 2010;58:4325–31.
[35] Ardell AJ, Kim DM, Ozolins V. Ripening of $L1_2$ Ni_3Ti precipitates in the framework of the trans-interface diffusion-controlled theory of particle coarsening. Z Metallkd 2006;97:295–302.

[36] Ardell AJ. A1–$L1_2$ interfacial free energies from data on coarsening in five binary Ni alloys, informed by thermodynamic phase diagram assessments. J Mater Sci 2011;46:4832–49.
[37] Li X, Thornton K, Nie Q, Voorhees PW, Lowengrub JS. Two- and three-dimensional equilibrium morphology of a misfitting particle and the Gibbs–Thomson effect. Acta Mater 2004;52:5829–43.
[38] Sequeira AD, Calderon HA, Kostorz G, Pedersen JS. Bimodal size distributions of γ′ precipitates in Ni–Al–Mo—II. Transmission electron microscopy. Acta Metall Mater 1995;43:3441–51.
[39] Lund AC, Voorhees PW. A quantitative assessment of the three-dimensional microstructure of a γ–γ′ alloy. Philos Mag 2003;83:1719–33.
[40] Swalin RA, Martin A. Solute diffusion in nickel-base substitutional solid solutions. Trans TMS-AIME 1956;206: 567–72.
[41] Guo Z, Sha W. Quantification of precipitation hardening and evolution of precipitates. Mater Trans 2002;43:1273–82.